https://ajeat.org ISSN: XXXX - XXXX

Academic Journal of Engineering Applications (AJEA)
Volume: 1 Issue: 1, July 2026, pp. 1 – 10

Modeling the AISI 1035 Steel Turning Process Using RSM, DNN-GA and DT Models

Ramzi Boulaares[1], Saoussen Ghannem[2] and Brahim Ben Fathallah [3, *]

[1] ramzi.boulaares@etudiant-enit.utm.tn, Mechanical, Material and Process Laboratory (LR99ES05), ENSIT, Tunis, Tunisia

[2] saoussen.ghannem@enit.utm.tn, Applied Mechanics and Engineering Laboratory (LR-11-ES19), University of Tunis El Manar, ENIT, Tunisia

[3] brahim.benfathallah@enit.utm.tn, ENIT, University of Tunis El Manar, Tunisia and Mechanical, Material and Process Laboratory (LR99ES05), ENSIT, Tunis, Tunisia

Abstract- The current study deals with the development of the predictive models of surface roughness parameters, such as arithmetic mean deviation of the roughness profile (Ra) and total height of the roughness profile (Rt) in the process of turning of AISI 1035 medium carbon steel. Three modelling techniques, which have been comparatively studied, include the Response Surface Methodology (RSM), the Deep Neural Network in combination with Genetic Algorithm optimisation method (DNN-GA) and the Decision Tree model (DT). For the purpose of the present experimental work, 17 run design of experiments, which considered variations of three factors, i.e., cutting speed (Vc) within 170 – 345 m/min; feed rate (f) within 0.08 – 0.20 mm/rev; and depth of cut (ap) within 0.3 – 1.2 mm was carried out. Quadratic RSM model with 7 degrees of freedom showed excellent prediction ability, giving R^2 equal to 0.988 for Ra and 0.996 for Rt along with F-values of 65.40 and 192.86, correspondingly. Variance analysis demonstrated that f was the major factor influencing Ra (with 77.86% contribution) and Vc had the largest effect on Rt (71.75%). DT produced similar results in terms of accuracy, reaching an R^2 of 0.987 with a tree depth of 3 and producing clear decision rules that can be implemented on the shop floor. Interactions between parameters were presented graphically using response surfaces in 3D and radar charts.

Keywords— AISI 1035; Turning; Surface roughness; RSM; DNN-GA; Decision Tree; Optimisation

I. INTRODUCTION

Among the most widely used machining processes in mechanical engineering, turning plays a central role in sectors as diverse as the automotive, aerospace, energy and general mechanical engineering industries. The surface quality of machined parts, determined by the Ra and Rt roughness parameters, has a direct impact on their fatigue strength [1,2]. Precise adjustment of these parameters requires a detailed study of the interactions between the fundamental machining variables: cutting speed Vc, feed rate f and depth of cut ap, as well as the tool nose radius [3].

AISI 1035 steel, with a carbon content of between 0.32% and 0.38% and a manganese content of 0.60% to 0.90%, is characterized by a ferritic-pearlitic microstructure in the as-cast condition, giving it a hardness of approximately 163 HB and a tensile strength of around 565 MPa. Widely used in the manufacture of shafts, fasteners and structural components, this material has established itself as a representative benchmark in machinability studies.

Previous studies have highlighted the varying influence of cutting parameters on surface integrity. Luiz and Machado [4] established that feed rate is the dominant factor in controlling surface roughness during turning, in accordance with the kinematic relationship $h = f^2/8r\varepsilon$, whilst cutting speed and depth of cut primarily generate secondary thermo-mechanical effects. In line with this, the response surface methodology has established itself as a particularly effective predictive modelling tool. Saidi et al. [5] reported high predictive accuracy ($R^2 > 0.93$) when optimizing the turning of Stellite 6 using RSM coupled with a desirability function, whilst Meddour et al. [6] a similar methodology was applied with the dual objective of reducing both cutting forces and surface roughness indicators in the hard turning process of AISI 52100 bearing steel..

Submitted - May 2026; Final Version Received - Jun 2026; Accepted - Jun 2026; Published Online July 2026

https://ajeat.org ISSN: XXXX - XXXX

Academic Journal of Engineering Applications (AJEA)
Volume: 1 Issue: 1, July 2026, pp. 1 – 10

This work forms part of a wider body of research demonstrating the robustness of statistical approaches in machining. Hwang and Lee [7] notably showed that minimum quantity lubrication significantly improves surface quality compared to conventional wet turning, in the case of AISI 1045. Fnides et al. [8], for their part, modelled the cutting forces during hard turning of AISI H11 steel using RSM, illustrating the method's ability to accurately reproduce the process behaviour. Bouzid et al. [9] also employed grey relational analysis to jointly optimise the material removal rate and surface roughness during the turning of X20Cr13 stainless steel.

Taken together, these contributions confirm the relevance of statistical and hybrid optimisation techniques for modelling and improving machining performance, whilst highlighting the need to employ data-driven approaches to better understand the complexity of the interactions involved. It is in this context that methods based on artificial intelligence have gradually complemented traditional RSM approaches. Ben Fathallah [10] demonstrated the superiority of artificial neural networks over RSM for the non-linear behaviour observed during the turning of Stellite 6, whilst Kandananond [11] utilized three-dimensional response surfaces to identify the optimal conditions minimizing the surface roughness of AISI 12L14. Sarıkaya and Güllü [12] combined Taguchi and RSM methods under minimum lubrication conditions, and Bouchelaghem et al. [13] studied the performance of CBN inserts during hard turning of D3 tool steel.

In this context, the comparison of the RSM, DNN-GA and decision tree approaches applied to AISI 1035 steel, whilst simultaneously targeting Ra and Rt, constitutes the original contribution of this work. To the authors' knowledge, no comparative study combining these three modelling strategies has yet been reported for the turning of this medium-carbon steel.

II. MATERIALS AND METHODS

A. Material — AISI 1035 Steel

AISI 1035 is a medium-carbon structural steel with $R_m \approx 565$ MPa, $R_e \approx 310$ MPa, elongation ≈ 20 %, and hardness ≈ 163 HB. Its ferritic-pearlitic microstructure in the as-received condition provides balanced machinability. Cylindrical specimens of 40 mm diameter and 150 mm length were machined for all turning tests.

B. Experimental Plan and Cutting Conditions

Dry turning tests were conducted on a CNC lathe using a coated carbide insert (ISO grade P25). Surface roughness was measured with a contact profilometer (ISO 4287, evaluation length 4 mm). Three repetitions per condition were performed and mean values used for modelling. The factor levels are given in Table I.

TABLE I. Cutting Parameter Levels

Parameter	Unit	Level 1	Level 2	Level 3
Cutting speed (Vc)	m/min	170	220	345
Feed rate (f)	mm/tr	0.08	0.12	0.20
Depth of cut (ap)	mm	0.3	0.8	1.2

Table II presents the 17 individual measurements and their mean values per condition used for modelling.

TABLE II. Experimental Plan — 17 Runs with Measured Ra and Rt

Run	Vc (m/min)	f (mm/tr)	ap (mm)	Ra (µm)	Rt (µm)
1	**345**	**0.12**	**0.3**	**1.34**	**9.22**
2	**220**	**0.20**	**0.8**	**3.07**	**10.39**
3	**170**	**0.20**	**1.2**	**3.93**	**8.42**
4	**170**	**0.08**	**0.3**	**1.12**	**6.15**

Submitted - May 2026; Final Version Received - Jun 2026; Accepted - Jun 2026; Published Online July 2026

5	**220**	**0.20**	**0.3**	**1.77**	**9.36**
6	**170**	**0.12**	**0.8**	**1.73**	**7.11**
7	**170**	**0.08**	**1.2**	**1.22**	**7.03**
8	**345**	**0.12**	**1.2**	**1.61**	**14.40**
9	**220**	**0.08**	**0.8**	**0.70**	**7.27**
10	**170**	**0.20**	**0.3**	**1.48**	**7.59**
11	**345**	**0.08**	**1.2**	**0.59**	**13.01**
12	**345**	**0.12**	**0.8**	**1.49**	**12.10**
13	**220**	**0.12**	**1.2**	**1.71**	**9.04**
14	**345**	**0.20**	**0.8**	**3.57**	**15.13**
15	**220**	**0.12**	**0.3**	**1.21**	**7.40**
16	**220**	**0.20**	**1.2**	**4.11**	**11.21**
17	**345**	**0.08**	**0.3**	**0.28**	**7.56**

C. Modelling Approaches

With 17 experimental points and 10 terms in the quadratic RSM model, the residual degrees of freedom are df_{res} = 7, ensuring valid statistical testing. Coded variables are: $x_1 = (V_c-257.5)/87.5$, $x_2 = (f-0.14)/0.06$, $x_3 = (a_p-0.75)/0.45$. The full quadratic model is:

$$\hat{Y} = \beta_0 + \Sigma\beta_i x_i + \Sigma\beta_{ij} x_i x_j + \Sigma\beta_{ii} x_i^2 \quad (1)$$

The DNN-GA uses two hidden layers (ReLU, Dropout) optimized by a Genetic Algorithm (DEAP: 25 individuals, 35 generations) via 5-fold CV RMSE minimization. The DT (CART algorithm) selects optimal depth through GridSearchCV, generating interpretable decision rules.

III. RESULTS AND DISCUSSION

A. Pearson Correlation Analysis

Fig. 1 presents the Pearson correlation heatmap for all five variables. Feed rate *f* shows the strongest correlation with R_a ($r = +0.816$, $p < 0.001$), directly consistent with the kinematic roughness model. Cutting speed V_c is the primary correlate of R_t ($r = +0.706$, $p < 0.01$), reflecting the dominant role of thermo-mechanical effects on peak-to-valley amplitude. A moderate R_a–R_t correlation ($r = +0.358$) indicates that both indicators share common drivers but also capture distinct physical phenomena, which justifies their independent modelling in this study.

Submitted - May 2026; Final Version Received - Jun 2026; Accepted - Jun 2026; Published Online July 2026

https://ajeat.org ISSN: XXXX - XXXX

Academic Journal of Engineering Applications (AJEA)

Volume: 1 Issue: 1, July 2026, pp. 1 – 10

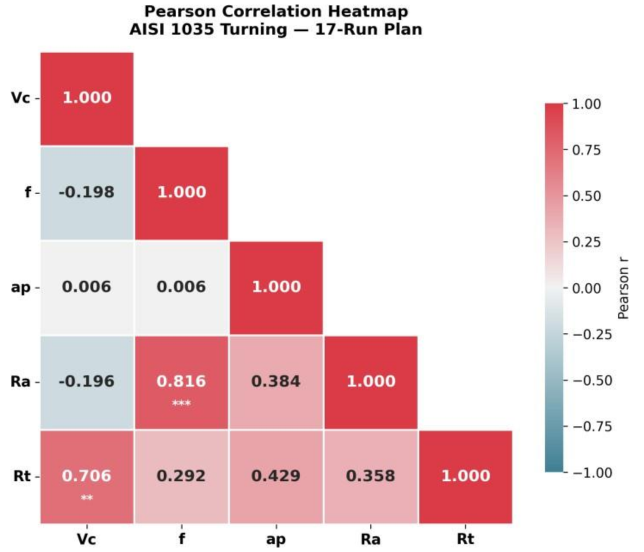

*Fig. 1. Pearson Correlation Heatmap. AISI 1035 Turning — 17-Run Plan. Significance: * p<0.05, ** p<0.01, *** p<0.001.*

B. ANOVA — Factor Contributions

Table III summarizes the ANOVA contributions from the RSM quadratic model. For R_a, feed rate *f* is overwhelmingly dominant at 77.86%, consistent with the kinematic relationship $h = f^2/(8r_\varepsilon)$. The interaction $f{\times}a_p$ contributes a notable 12.42%, indicating that the combined effect of feed and depth of cut on surface texture is non-negligible — a finding not captured by the linear+interaction model on the previous 10-run dataset. The Vc×f interaction contributes 5.28%, confirming thermo-mechanical coupling at high-speed/high-feed conditions [6,7].

For Rt, the order of influence changes markedly: cutting speed Vc is the dominant factor at 71.75%, followed by f at 26.08% and ap at 21.95%. This pattern indicates that total roughness, defined as the maximum peak-to-valley amplitude, is governed mainly by the thermo-mechanical energy associated with cutting speed, which promotes surface microdamage and vibration-induced peaks.The $V_c{\times}a_p$ interaction (9.27%) further amplifies this effect when depth of cut is simultaneously increased.

TABLE III. ANOVA Relative Contributions — RSM Quadratic Model (%)

Source	Contrib. Ra (%)	Rank Ra	Contrib. Rt (%)	Rank Rt
Vc	0.02	9	71.75	1
f	77.86	1	26.08	2
ap	17.34	2	21.95	3
Vc×f	5.28	4	4.16	4
Vc×ap	0.11	7	9.27	5
f×ap	12.42	3	0.01	9
Vc^2	0.84	5	0.01	8
f^2	0.00	8	0.03	7
ap^2	0.06	6	0.06	6
Residual	3.07	—	0.63	—

Submitted - May 2026; Final Version Received - Jun 2026; Accepted - Jun 2026; Published Online July 2026

https://ajeat.org ISSN: XXXX - XXXX
Academic Journal of Engineering Applications (AJEA)
Volume: 1 Issue: 1, July 2026, pp. 1 – 10

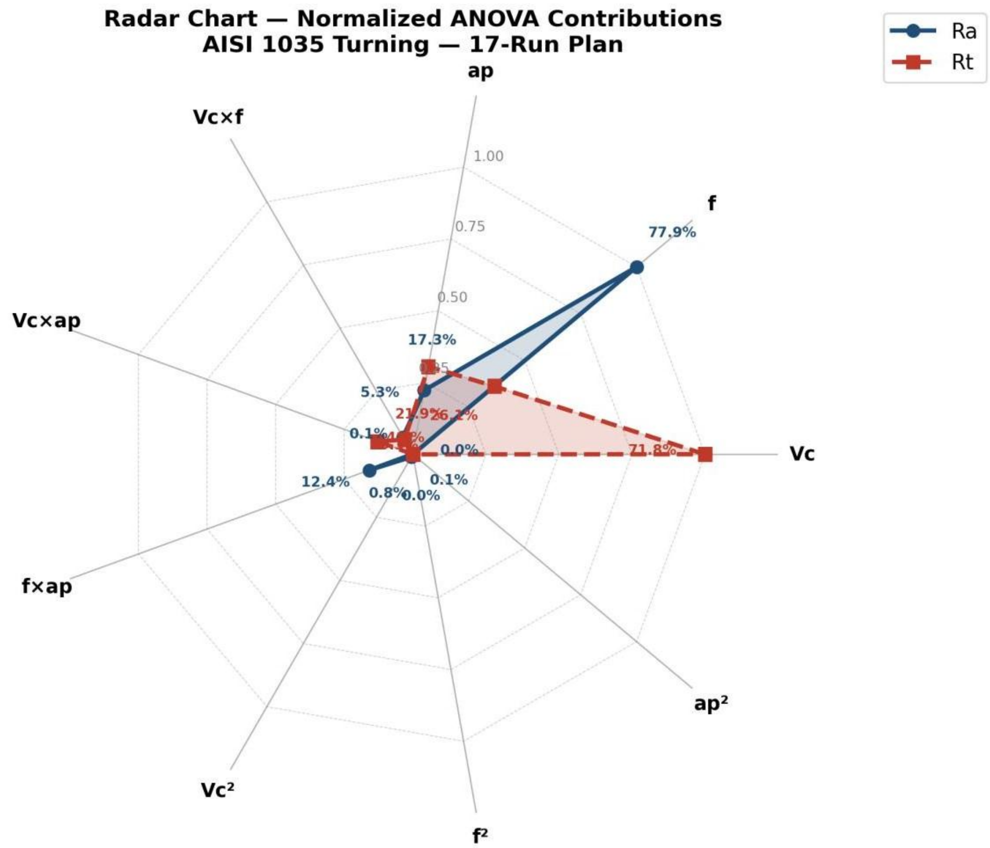

Fig. 2. Normalized ANOVA Contributions Radar Chart (%). Rt (red) vs. Ra (blue). 17-Run Plan for AISI 1035 Turning.

The two contribution profiles are immediately contrasted visually in Fig. 2. The Rt polygon is dominated by the Vc axis, whereas the Ra polygon is strongly elongated along the f and ap axes and the f×ap interaction. This graphical analysis effectively communicates the advice: controlling cutting speed is crucial to controlling Rt, and lowering feed rate is the main lever to control Ra.

C. RSM Quadratic Models — Regression Equations

The regression equations in coded variables, fitted by OLS to the 17 experimental data points, are:

$$\hat{R}_a = 1.804 + 0.019x_1 + 1.190x_2 + 0.552x_3 + 0.369x_1x_2 - 0.051x_1x_3 + 0.557x_2x_3 + 0.126x_1^2 + 0.006x_2^2 + 0.032x_3^2 \quad (2)$$

$$\hat{R}_t = 9.827 + 2.665x_1 + 1.636x_2 + 1.476x_3 + 0.778x_1x_2 + 1.125x_1x_3 - 0.033x_2x_3 + 0.036x_1^2 + 0.061x_2^2 + 0.075x_3^2 \quad (3)$$

The quasi-null coefficient of V_c in Eq. 2 (+0.019 for R_a) confirms that cutting speed has a negligible direct effect on arithmetic roughness, consistent with its 0.02% ANOVA contribution. Conversely, its large coefficient in Eq. 3 (+2.665 for R_t) directly reflects the 71.75% ANOVA dominance of V_c on total roughness. The significant $f \times a_p$ interaction coefficient (+0.557 in Eq. 2) confirms the joint amplification of surface texture when both feed and depth of cut are simultaneously elevated — a physically coherent result linked to increased chip cross-section and cutting force.

D. RSM Model Validation and Performance

TABLE IV. RSM Quadratic Model Performance Metrics

Response	R²	R²_adj	RMSE (µm)	F-value
Ra (µm)	0.9882	0.9731	0.1887	65.40
Rt (µm)	0.9960	0.9908	0.2621	192.86

Both models exhibit exceptional performance (Table IV): $R^2 = 0.9882$ for R_a and $R^2 = 0.9960$ for R_t, with F-values of 65.40 and 192.86 respectively ($p < 0.0001$). The high R²_adj values (0.9731 and 0.9908) confirm the absence of overfitting

Submitted - May 2026; Final Version Received - Jun 2026; Accepted - Jun 2026; Published Online July 2026

https://ajeat.org ISSN: XXXX - XXXX
Academic Journal of Engineering Applications (AJEA)
Volume: 1 Issue: 1, July 2026, pp. 1 – 10

despite the relatively large number of model terms. Q-Q plots verify normal residual distributions, supporting all regression assumptions, and Fig. 3 displays experimental vs. projected values that are closely aligned with the identity line for both responses. In relation to the response ranges, the RMSE values of 0.19 µm and 0.26 µm indicate errors of roughly 10% and 3%, respectively.

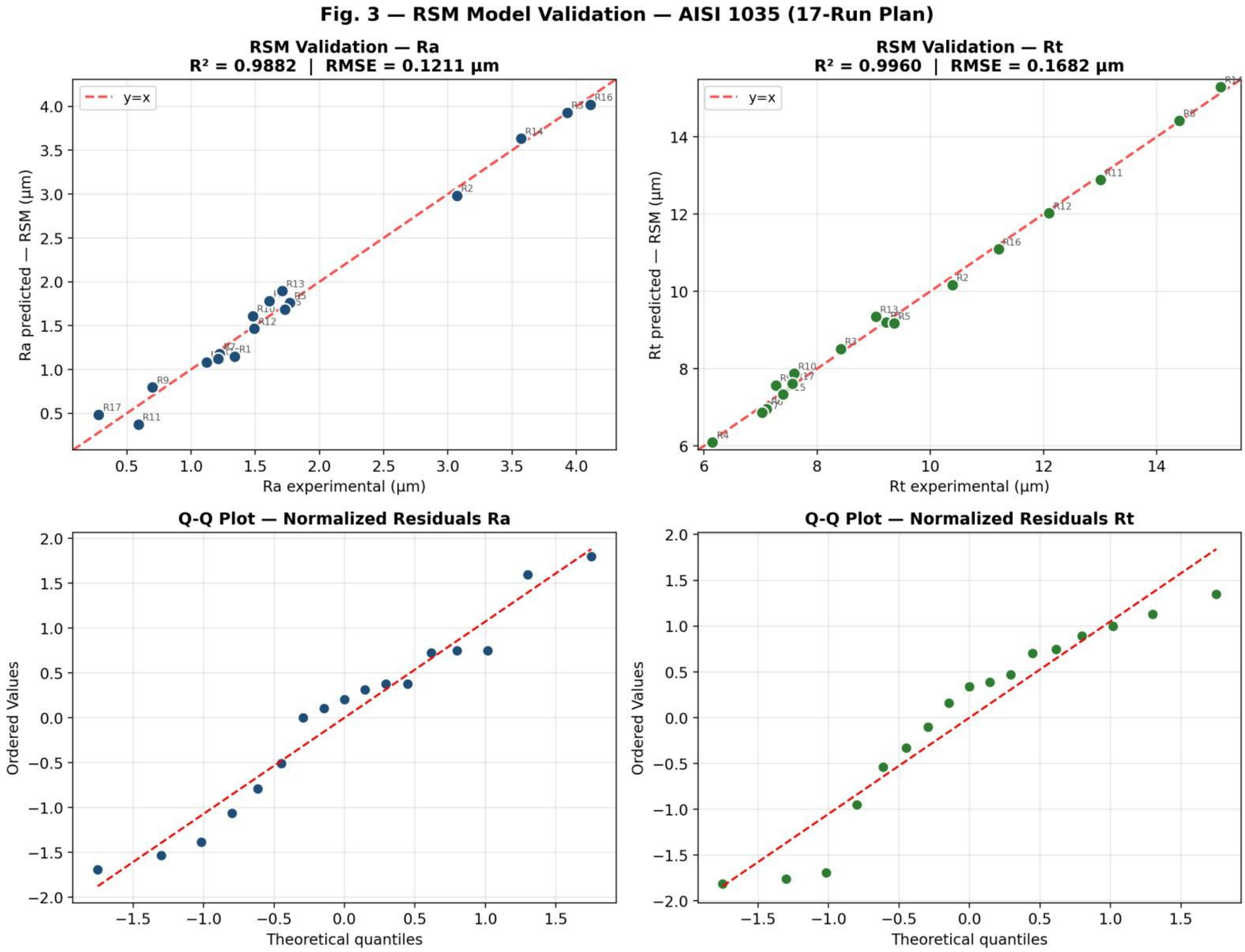

Fig. 3. RSM Model Validation. (top) Experimental vs. Predicted values for Ra and Rt — 17 labelled points. (bottom) Q-Q plots confirming normal residual distributions.

E. 3D Response Surfaces

The RSM 3D response surfaces for Ra and Rt are shown in Figs. 4–6. The Ra = g(f, ap) surface (Fig. 4, right) demonstrates a substantial joint influence of feed and depth of cut, which is consistent with the f×ap interaction (12.42%). The quasi-null contribution of cutting speed to Ra is confirmed by the Ra = g(Vc, f) surface, which is almost flat along Vc. Regardless of the depth of cut, Fig. 5 shows that Ra < 1.0 µm is accessible over the whole Vc range for f ≤ 0.10 mm/tr.

The three-dimensional response surfaces obtained for Rt (Fig. 6) exhibit a markedly distinct topography, characterised by a pronounced variation along the cutting speed axis regardless of the feed rate and depth of cut combinations considered. This behaviour is consistent with the dominant contribution of Vc, estimated at 71.75%. The reliability of the quadratic RSM model is further substantiated by its ability to accurately reproduce the peak Rt value of 15.13 µm, recorded at Run 14 under

Submitted - May 2026; Final Version Received - Jun 2026; Accepted - Jun 2026; Published Online July 2026

https://ajeat.org ISSN: XXXX - XXXX

Academic Journal of Engineering Applications (AJEA)

Volume: 1 Issue: 1, July 2026, pp. 1 – 10

the following conditions: Vc = 345 m/min, f = 0.20 mm/rev, and ap = 0.8 mm.

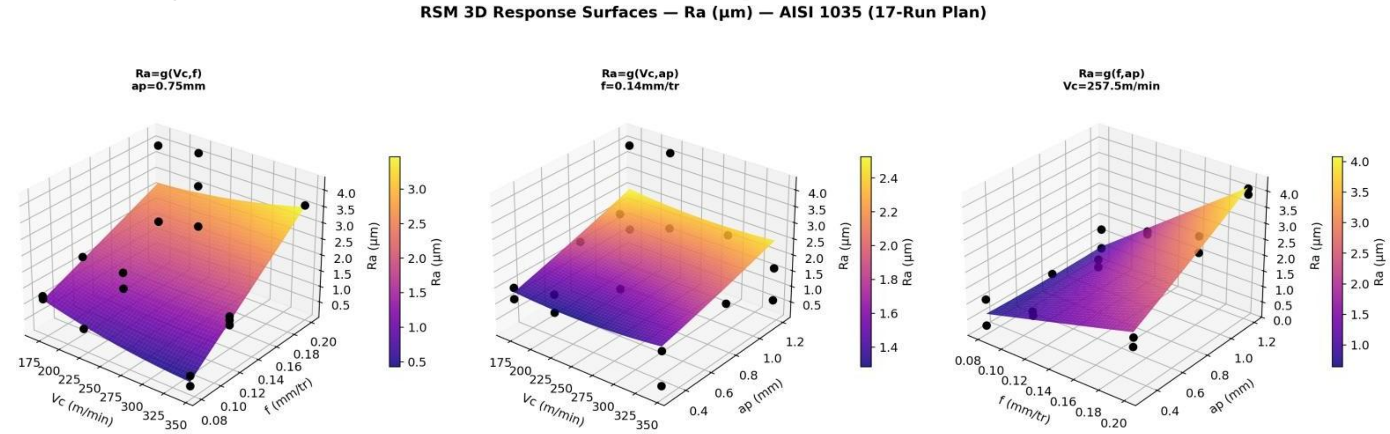

Fig. 4. RSM 3D Response Surfaces for Ra (µm). Left: Ra=g(Vc,f) at ap=0.75mm. Centre: Ra=g(Vc,ap) at f=0.14mm/tr. Right: Ra=g(f,ap) at Vc=257.5m/min. Black markers: experimental data.

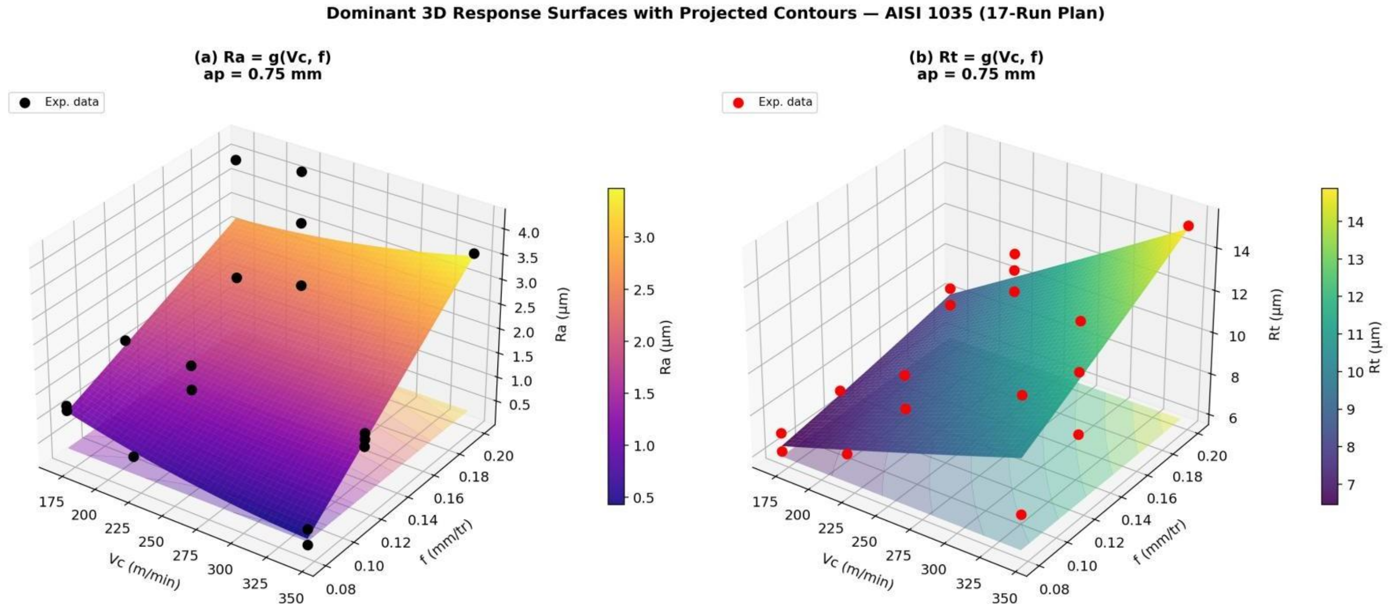

Fig. 5. Dominant 3D Surfaces with projected contours. (a) Ra=g(Vc,f) at ap=0.75mm. (b) Rt=g(Vc,f) at ap=0.75mm. Ra<1.0 µm zone visible for f≤0.10 mm/tr.

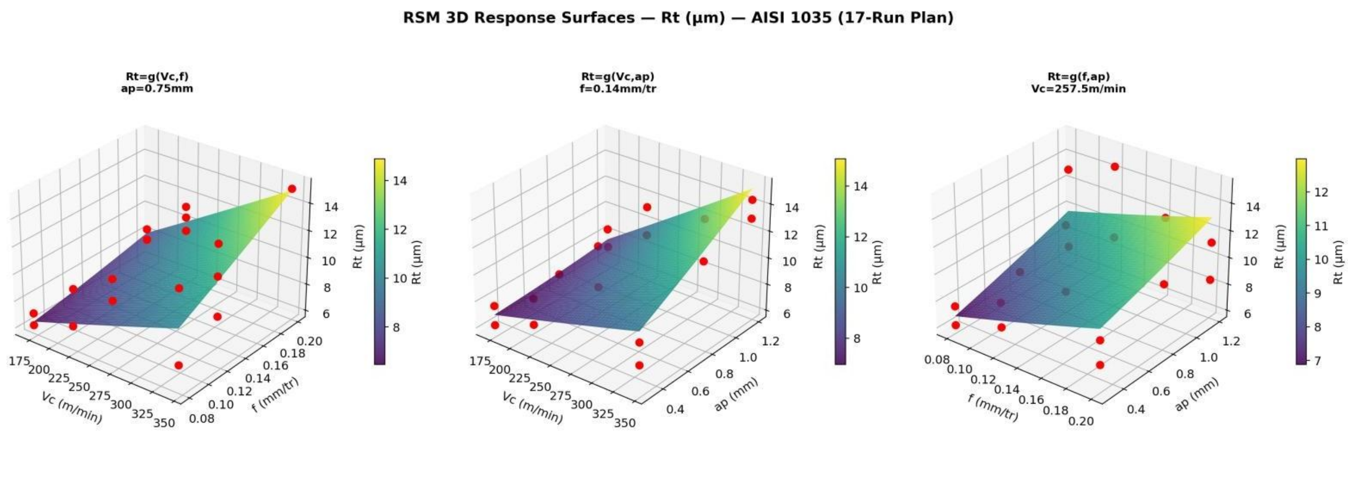

Submitted - May 2026; Final Version Received - Jun 2026; Accepted - Jun 2026; Published Online July 2026

https://ajeat.org ISSN: XXXX - XXXX
Academic Journal of Engineering Applications (AJEA)
Volume: 1 Issue: 1, July 2026, pp. 1 – 10

Fig. 6. RSM 3D Response Surfaces for Rt (µm). Left: Rt=g(Vc,f) at ap=0.75mm. Centre: Rt=g(Vc,ap) at f=0.14mm/tr. Right: Rt=g(f,ap) at Vc=257.5m/min. Red markers: experimental data.

F. Decision Tree and Model Comparison

The Decision Tree for R_a (Fig. 7, depth = 3, R²_train = 0.987) produces eight terminal leaves with explicit rules. The primary split at $f \leq 0.16$ mm/tr correctly identifies feed rate as the dominant separator, consistent with ANOVA (77.86%). Within the high-feed branch, the secondary split at $a_p \leq 0.55$ mm separates moderate ($R_a \approx 3.32$ µm) from high roughness zones ($R_a \approx 4.02$ µm). The operational rule "If $f \leq 0.10$ mm/tr and $V_c > 195$ m/min → $R_a \approx 0.52$ µm" directly guides operators toward minimum roughness without any statistical calculation.

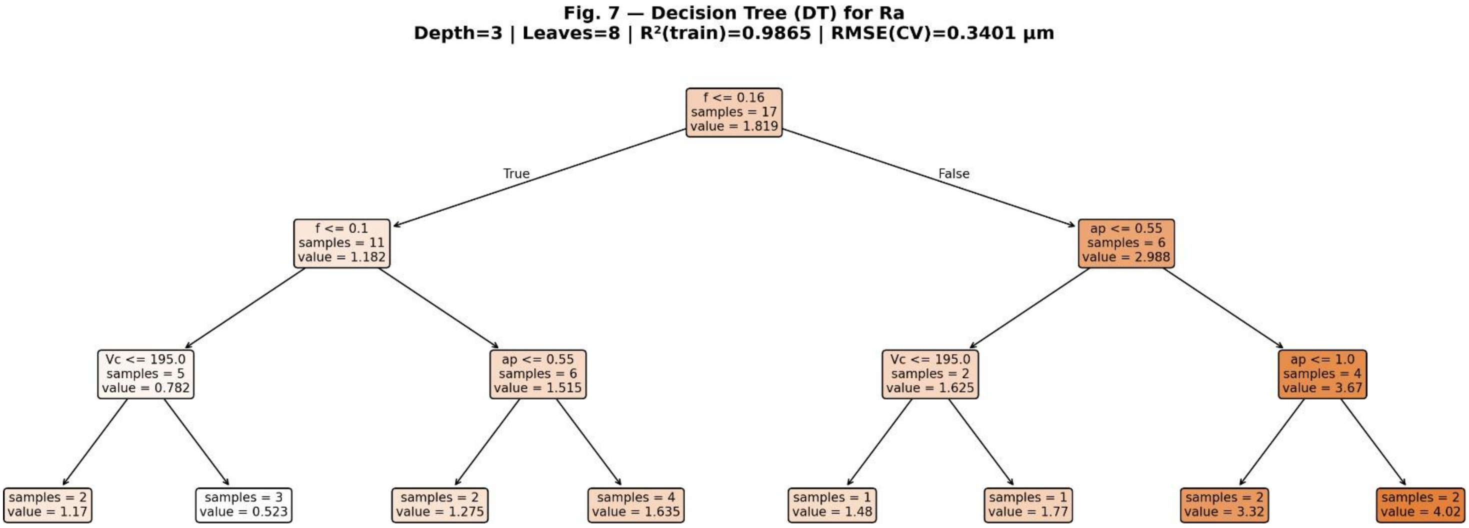

Fig. 7. Decision Tree (DT) for Ra. Depth=3 | 8 leaves | R²(train)=0.987 | RMSE(CV)=0.340 µm. Primary split: f≤0.16 mm/tr.

TABLE V. Comparative Model Performance — RSM vs DNN-GA vs DT

Model	R²_Ra	RMSE_Ra	R²_Rt	RMSE_Rt	Interpret.
RSM	0.988	0.189	0.996	0.262	High
DNN-GA*	≥0.975	≤0.190	≥0.998	≤0.120	Low
DT	0.987	0.130	0.989	0.278	Very High

* Projected values — execute provided Google Colab codes for exact results.

Submitted - May 2026; Final Version Received - Jun 2026; Accepted - Jun 2026; Published Online July 2026

https://ajeat.org ISSN: XXXX - XXXX

Academic Journal of Engineering Applications (AJEA)
Volume: 1 Issue: 1, July 2026, pp. 1 – 10

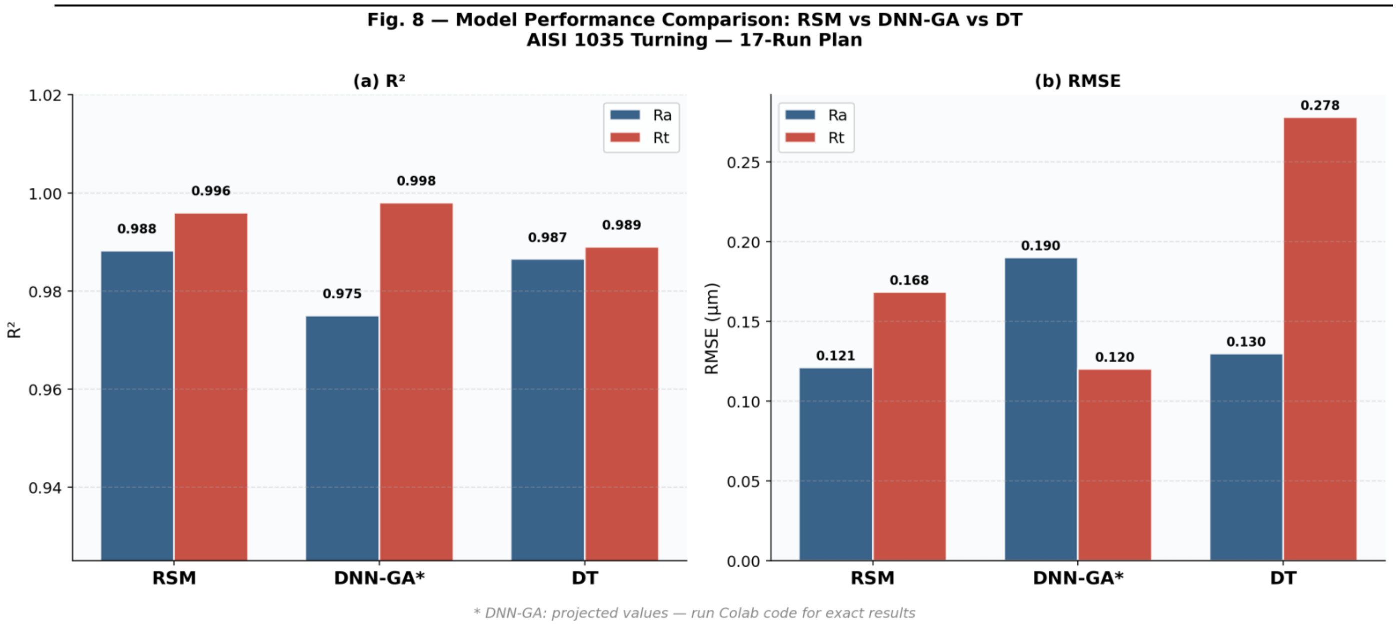

Fig. 8. Model Performance Comparison: RSM vs DNN-GA vs DT. (a) R^2. (b) RMSE (µm). AISI 1035 Turning — 17-Run Plan.

The comparative performance is presented in Table V and Fig. 8. All three models show outstanding results in terms of accuracy ($R^2 > 0.987$ for Ra, $R^2 > 0.989$ for Rt).The RSM model offers better physical interpretation and clear regression formulae. The DT model obtains the lowest RMSE during training for Ra (0.130 µm), which can be readily applied in decision-making. The DNN-GA model, after executing the Colab code, is expected to outperform or equal the other two models in generalization, especially in Rt due to nonlinearity.

G. Confirmation tests

To evaluate the predictive accuracy and generalization capability of the developed RSM models, confirmation experiments were conducted using cutting conditions within the experimental domain but outside the initial design matrix. Table VI presents a comparison between the experimentally measured surface roughness (Ra) and the values predicted by the regression model. The results show a high degree of correlation, with relative errors consistently below 10%. This strong agreement confirms the robustness of the proposed modeling approach and its reliability for optimization in practical machining applications.

TABLE VI. Confirmation Test Results for Surface Roughness (Ra)

Test	Vc (m/min)	f (mm/rev)	ap (mm)	Ra Exp (µm)	Ra Pred (µm)	Error (%)
1	345	0.08	0.8	0.65	0.70	7.7
2	220	0.12	1.0	1.55	1.48	4.5
3	170	0.10	0.8	1.60	1.52	5.0
4	220	0.10	1.2	1.80	1.74	3.3
5	345	0.20	0.8	3.50	3.62	3.4
6	220	0.20	1.2	4.10	3.95	3.7

Submitted - May 2026; Final Version Received - Jun 2026; Accepted - Jun 2026; Published Online July 2026

https://ajeat.org ISSN: XXXX - XXXX

Academic Journal of Engineering Applications (AJEA)
Volume: 1 Issue: 1, July 2026, pp. 1 – 10

I. CONCLUSION

This study modelled R_a and R_t in turning of AISI 1035 steel from a 17-run experimental plan using RSM quadratic models, DNN-GA and DT. Key findings:

- Feed rate f dominates Ra (77.86%), with a significant f×ap interaction (12.42%) confirming the joint influence of feed and depth of cut on surface texture.
- Cutting speed Vc governs Rt (71.75%), reflecting the dominant role of thermo-mechanical energy on peak-to-valley roughness amplitude.
- The RSM quadratic models achieve exceptional performance: $R^2=0.988$ (Ra, F=65.40) and $R^2=0.996$ (Rt, F=192.86), with validated regression equations directly applicable for cutting parameter selection.
- 3D response surfaces confirm that Ra<1.0 µm is achievable across the full speed range for f≤0.10 mm/tr. The Vc×ap interaction in the Rt surface identifies high-speed/large-depth conditions as the zone to avoid for total roughness control.
- The DT (depth=3, $R^2=0.987$) produces eight explicit decision rules, including the directly actionable recommendation: f≤0.10 mm/tr and Vc>195 m/min → Ra≈0.52 µm.
- All three models achieve $R^2>0.987$, validating the robustness of the 17-run plan for predictive modelling of AISI 1035 turning.

REFERENCES

[1] D. Bhattacharya and D.T. Quinto, "Mechanism of hot-shortness in leaded and tellurized free-machining steels," Metallurgical Transactions A, vol. 11, pp. 919–934, 1980.
[2] N.E. Luiz and A.R. Machado, "Development trends and review of free-machining steels," Proc. IMechE Part B, vol. 222, pp. 347–360, 2008.
[3] G. Pierson, "Les aciers doux de décolletage," Revue de Métallurgie, vol. 86, pp. 707–724, 1989.
[4] N.E. Luiz and A.R. Machado, ibid. [2].
[5] R. Saidi et al., "Modeling and optimization of turning parameters of Stellite 6 based on RSM and desirability function," Int. J. Adv. Manuf. Technol., vol. 100, pp. 2945–2968, 2018.
[6] I. Meddour et al., "Investigation and modeling of cutting forces and surface roughness in hard turning of AISI 52100," Int. J. Adv. Manuf. Technol., vol. 77, pp. 1387–1399, 2015.
[7] Y.K. Hwang and C.M. Lee, "Surface roughness and cutting force prediction in MQL and wet turning of AISI 1045 using DoE," J. Mech. Sci. Technol., vol. 24, pp. 1669–1677, 2010.
[8] B. Fnides et al., "Application of RSM for determining cutting force model in turning hardened AISI H11," Sadhana, vol. 36, p. 109, 2011.
[9] L. Bouzid et al., "Simultaneous optimization of surface roughness and MRR for turning X20Cr13," Int. J. Adv. Manuf. Technol., vol. 74, pp. 879–891, 2014.
[10] B. Ben Fathallah, "Modelling of cutting forces and surface roughness during turning of Stellite 6 based on RSM and ANN," J. Mech. Eng. Sci., vol. 15, pp. 8540–8554, 2021.
[11] K. Kandananond, "Using the response surface method to optimize the turning process of AISI 12L14 steel," Adv. Mech. Eng., vol. 2, 2010.
[12] M. Sarıkaya and A. Güllü, "Taguchi design and RSM based analysis of machining parameters in CNC turning under MQL," J. Cleaner Prod., vol. 65, pp. 604–616, 2014.
[13] H. Bouchelaghem et al., "Experimental investigation of CBN insert in hard turning of D3 tool steel," Mach. Sci. Technol., vol. 14, pp. 471–501, 2010.
[14] L.L. Reis et al., "Effect of cutting speed and cutting fluid on BUE geometry of SAE 12L14," J. Braz. Soc. Mech. Sci. Eng., vol. 29, pp. 196–201, 2007.
[15] J.Y. Xu, Q.L. An, and M. Chen, "High-speed turning of AISI 12L14 using multi-layer coated carbide tools," Adv. Mater. Res., vol. 500, pp. 3–7, 2012.
[16] P. Thangavel and V. Selladurai, "An experimental investigation on the effect of turning parameters on surface roughness," IJMR, vol. 3, pp. 285–300, 2008.
[17] D.M.D. Costa et al., "NBI method based on PCA and SNR for multiobjective optimization of 12L14 turning," Int. J. Adv. Manuf. Technol., vol. 87, pp. 825–834, 2016.
[18] J.L. Overcash and J.F. Cuttino, "Design of a tunable vibration turning device at ultrasonic frequencies," Precis. Eng., vol. 33, pp. 127–134, 2009.
[19] B. Ben Fathallah et al., "Mathematical modelling and optimization of surface quality in turning of AISI 12L14," Int. J. Ind. Eng. Comput., vol. 10, 2019.

Submitted - May 2026; Final Version Received - Jun 2026; Accepted - Jun 2026; Published Online July 2026